Influence of Empty Space and Internal Stresses on Dielectric Strength in Two-phase Polymer

O. A. Lambri[(a)], F. Tarditti[(b)], J. A. Cano, G. I. Zelada
Laboratorio de Materiales (LEIM), Escuela de Ingeniería Eléctrica (EIE), Facultad de Ciencias Exactas, Ingeniería y Agrimensura (FCEIA), Universidad Nacional de Rosario (UNR), Av. Pellegrini 250, 2000, Rosario, Argentina
(a) Member of the CONICET's Research Staff. Instituto de Física Rosario, Rosario, Argentina
(b) CONICET's fellowship

J. A. García[(c)], D. Merida Sanz[(c)], F. Plazaola Muguruza[(d)]
Facultad de Ciencias y Tecnología, Universidad del País Vasco, UPV/EHU, Apdo. 644, 48080 Bilbao, País Vasco, Spain
(c) Departamento de Física Aplicada II
(d) Elektrika eta Elektronika Saila

C. E. Boschetti[(e)] and **G. E. Martínez Delfa**
Área de Tecnología Química, Facultad de Ciencias Bioquímicas y Farmacéuticas, Universidad Nacional de Rosario Suipacha 531, S2002LRK Rosario, Argentina
(e) Member of the CONICET's Research Staff

ABSTRACT

In the present work, a study on the dependence of the Dielectric Strength (DS) as a function of the empty space and the internal stresses into polymer samples has been performed. The empty space was measured by means of positron annihilation lifetime spectroscopy. The internal stresses into the polymer matrix, due to the appearance of the crystalline zones, were determined by applying the inclusion theory results to the dynamic mechanical analysis measurements. Attention to the effect of the chain movement on the electrical breakdown process has been paid. The study has been performed at a mesoscopic scale with the aim of demonstrating the influence of the thermal, mechanical or electrical stresses on the chains movement and their effect on the dielectric breakdown phenomenon. It has been verified that, DS is a function of the empty space into the sample and also of the internal stresses acting at the polymer chains, which result from the crystalline state promoted by chemicrystallization. The empty space decrease and the internal stresses act overlapped against the electrical force operating on the polymer chains. It is deduced from the work, that the precursor phenomenon for the electrical breakdown is the bend of polymer chains, prior to the onset of their collective movement promoted by the electrical forces.

Index Terms - **EPDM, molecular chain movements, electric breakdown, positron annihilation lifetime spectroscopy, dynamic mechanical analysis.**

1 INTRODUCTION

COMPOSITE polymeric insulators are widely used for applications at high voltages in both the distribution and transmission voltage ranges, due to their substantial advantage compared to inorganic insulators which have primarily been porcelain and glass. Their major advantages are their low surface energy, light weight, a higher mechanical strength to weight ratio, easy installation and the reduction of maintenance cost, among others; see for more details [1]. In addition, line post insulators are less prone to serious damage from vandalism such as gunshots, which cause the ceramic insulators to shatter and drop the conductor to the ground [1, 2]. However, the environmental effects lead to a critical aging of the polymer producing degradation in its physical, mechanical and electrical properties [1, 3, 4].

Several works focused on the study of the electric breakdown phenomenon of insulating materials and its corresponding driving force have been reported [1, 3, 5-14]. Electric breakdown occurs when the current flowing through the sample increases, leading to its failure and consequently, the applied voltage cannot be stable. The voltage, leading to the material disruption is called breakdown voltage, and the corresponding voltage gradient at failure is the dielectric strength (DS) [3, 5]. The understanding of

Manuscript received on 18 December 2012, in final form 26 April 2013.

the physical-chemical breakdown mechanisms is not yet complete, but one could distinguish the following processes: (a) intrinsic breakdown, which is related to the pure and defect-free material. It is due to the increased random motion of electrons, (b) thermal breakdown, which is related to the heat emission, (c) gas-discharge dependent breakdown, which is related to electric discharges in gas and may occur on the surface of voids and/or various discontinuities of the electrical insulator, (d) physical dependent breakdown, which is affected by cracks, voids, foreign inclusions and by factors that introduce physical deterioration of polymers [3, 5, 10, 11].

Electrical treeing is another mechanism, which may lead to electrical breakdown. Treeing is related to sporadic discharges that are intermittent and not steady like corona discharge. The mechanism of treeing is very similar to electric breakdown [5]. In fact, treeing breakdown starts in the regions with the highest and most divergent electrical stresses [5, 8, 13]. The practical importance of treeing has been emphasized in many cases, particularly for polyethylene cables [5, 13]. In other works the fractal properties of the branched discharges have been proposed [15]. In addition, many studies in non-ceramic insulators reflect the importance of the dry-band-arcing phenomenon. Dry band arcing at currents as low as 1 to 20 mA may be responsible for surface erosion of non-ceramic insulators. At these currents the relatively stable arc-roots, at localized regions of reduced resistance, are able to inject significant energy into the non-ceramic material. Corona and dry band arcing are very different mechanisms, since corona is a field related phenomenon, while dry band arcing is a leakage current related one. Dry band arcing can only happen once hydrophobicity has been lost, since a hydrophobic surface will have no leakage currents [7].

A very used rubber for the housing of the mechanical resistant core of the polymeric electrical insulators is EPDM (ethylene-propylene-diene M-class rubber). In this polymer, the outdoor ageing leads to a loss of hydrophobicity and also to the decrease of the volume fraction and the size of the crystallites [4]. In addition, it has been already reported that volume fraction of the crystalline zones in EPDM and the size of the crystallites can be modified by neutron irradiation [16-19]. Indeed, neutron irradiation on EPDM leads to the increase in the crystalline degree of this semicrystalline polymer, through a process of chemicrystallization, which depends on dose and neutron flux level [16-19].

In the present work, the dependence of DS with both the degree of empty space in the sample, determined by means of positron annihilation lifetime spectroscopy (PALS) and the internal stresses into the polymer matrix, due to the appearance of the crystalline zones, determined by applying the inclusion theory results to dynamic mechanical analysis (DMA) measurements, has been studied. Attention to the effect of the chain movement related to the breakdown process has been paid. In fact, the study has been performed at a mesoscopic scale with the aim of demonstrating the influence of the thermal, mechanical or electrical stresses on the chain movement and their effect on the dielectric breakdown phenomenon. As it will be shown along the work, this way of studying the breakdown phenomenon brings out new tools to the characterization of the electrical breakdown in semi-crystalline polymers.

2 THEORETICAL BACKGROUND: ELASTIC MISFIT FOR AN INCLUSION SMALLER THAN THE HOLE IN THE MATRIX

In this Section, the concepts and equations related to the misfit of strain in a semi-crystalline polymer for the case of an inclusion having a size smaller than the hole in the matrix where it is located, have been developed [18]. This situation is more complex than the one consisting of an inclusion larger than the size of the matrix hole, and it will be here developed since this situation applies to the present work. The main concepts to take into account for this case are summarized in Figure 1. In this paper the one-dimensional case will be developed; see for more details [18, 19]. The model takes the idea of partitioning the volume of the sample in small elementary cubes in such a way that each partitioned element is composed by a single phase (amorphous or crystalline in the polymer material we are dealing with) [19, 20]. The crystallites are here the inclusions embedded into a continuous and homogeneous matrix, which is represented by the amorphous phase of the polymer. Figure 1, shows a (z,y) plane of the partitioned sample at x = v, where the size of the partitioned matrix, over each axis, was chosen equal to lo_p. The model now starts with the following considerations:

a) The volume element located at (v,m,j) of the whole partitioned matrix, which is plotted by means of full fine lines in Figure 1, is cut and removed out of the matrix; leading to a cubic hole of side lo_p.

b) An inclusion of size $lo_p - \in lo_p$, with $0 \leq \in \leq 1$, plotted by means of broken lines will be placed into the hole of the matrix, surrounded by glue, and then the matrix is compressed up to the inclusion integrates into the matrix.

c) The stress is mechanically released and then the boundaries of the hole, in the x, y and z axes, displace to a position $lo_p - \beta \in lo_p$, with $0 \leq \beta \leq 1$, where the equilibrium of stresses is achieved. The wider lines in Figure 1 represent this state. β is called the strain misfit coefficient.

We will consider, the movement of the boundary in the z-axis, produced by the inclusion located at (v,m,j) and its effects over the neighbor matrix element (v,m,k), Figure 1. The displacement of the boundary of the element (v,m,j) from the initial position (cube in dashed line in Figure 1) after the inclusion is pasted to the matrix and released, achieving the mechanical equilibrium, leads to the movement of the front part face along the z direction, from the narrow solid line to the wider line, Figure 1.

Hereafter, the magnitudes corresponding to the inclusion or to the matrix, will be noted with a subscript i or m, respectively. In addition, in order to keep the same style of the mathematical notation used in previous works [18, 19], either the direction for the strain misfit coefficient, β, and for the number of inclusions or matrix elements (N) will be denoted through a suprasubscript.

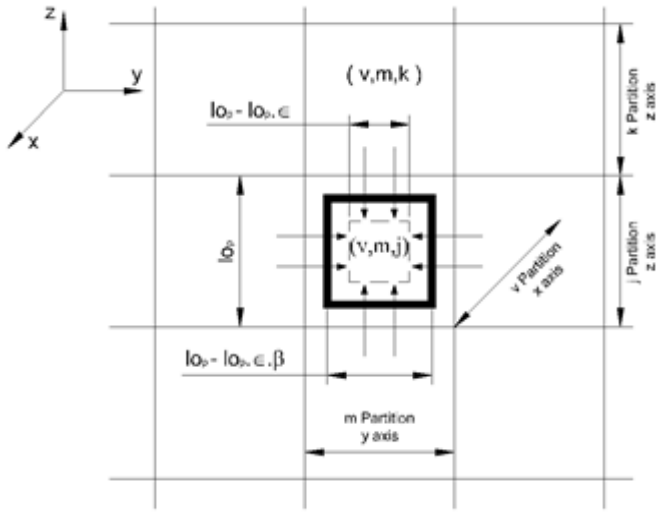

Figure 1. Accommodation of the misfit strain by the appearance of an inclusion into the material matrix, for the case: inclusion smaller in size than the size of the hole. Fine full line: Initial size of the base of the cube of the partitioned material. Broken line: Size of the inclusion free of stresses. Wider full line: Equilibrium position of the boundary between the inclusion and the matrix, after location of the inclusion into the matrix hole (see details in the text). Arrows in the Figure indicate the stretching effect of the inclusion on the matrix. Taken from [18].

Then, as it is shown in [18, 19], the displacement in the z-axis, $u_i(z)$, is

$$u_i(z) = \left(z - z.\in.\beta^z \right) - \left(z - z.\in \right) \tag{1}$$

$$u_i(z) = z \in \left(1 - \beta^z \right) \tag{2}$$

Consequently the mean strain inside the inclusion (averaged by the mean field approximation) in the z-axis, ε_i^z, results,

$$\varepsilon_i^z = \frac{\partial u_i}{\partial z} = \in \left(1 - \beta^z\right) \tag{3}$$

In order to calculate the resulting mean strain inside the matrix element, it will be considered that there exists an inclusion concentration lying in the z-axis N_i^z/N_m^z, where N_i^z and N_m^z are the number of inclusions and the number of matrix elements, respectively; which satisfy the condition $N_i^z + N_m^z = N^z$. The N_i^z inclusions move the boundaries of the N_m^z partitions, in such a way that it corresponds to the displacement $z + z \in \beta^z N_i^z/N_m^z$. Then, the displacement in the z-axis for the matrix elements can be written,

$$u_m(z) = z.\in.\beta^z \left(\frac{N_i^z}{N_m^z} \right) \tag{4}$$

Therefore, the strain inside the matrix element in the z-axis, ε_m^z, results,

$$\varepsilon_m^z = \frac{\partial u_m}{\partial z} = \in.\beta^z \left(\frac{N_i^z}{N_m^z} \right) \tag{5}$$

By working equation (5) we obtain,

$$\varepsilon_m^z = \in.\beta^z \left(\frac{N_i^z / N^z}{N_m^z / N^z} \right) = \in.\beta^z \left(\frac{fr_i^z}{fr_{m,}^z} \right) \tag{6}$$

Where fr_i^z and fr_m^z are the volume fraction for the inclusions and matrix element in the z axis, respectively; which verify that $(fr_i + fr_m) = 1$.

From the mechanical equilibrium conditions at the boundary between the adjacent elements (v,m,j) and (v,m,k), according to the Reuss approximation, [21] and by applying the Hooke's law; the misfitting coefficient in the z-axis, β^z, can be obtained as a function of the Young moduli, E, and volume fractions of both inclusions and matrix such that,

$$\beta^z = \frac{1}{1 + \left(\frac{E_m}{E_i} \right) \cdot \left(\frac{fr_i^z}{fr_m^z} \right)} \tag{7}$$

The procedure for obtaining from DMA tests, fr_i, fr_m, E_m and E_i has been described in previous works [19, 20].

Moreover, considering that the distribution of inclusions is random in the bulk matrix, it can be demonstrated easily that [19]

$$\beta^z = \beta^x = \beta^y = \beta \tag{8}$$

Indeed, β is the misfit coefficient, which relates the strain on the inclusion caused by the matrix (or vice-versa). The larger the strain over the inclusion, the lower the value of β, or vice-versa. Moreover, as it was shown in [18], the result for β when the inclusion is larger than the size of the hole, is equivalent to the one obtained in equation (7), since the absolute value for the displacements, equation (2), in both cases is the same.

3 EXPERIMENTAL

3.1 SAMPLES

Samples were taken from commercial EPDM used as housing of non-ceramic electrical insulators (Avator of Sitece Electrical Industries, Buenos Aires, Argentina), which are employed in outdoor transmission lines of 66 kV. EPDM composition was determined by means of IR spectroscopy, following directions of ASTM D 3900 standard [22]. The nominal molar composition of the rubber was 65% ethylene – 32% propylene and 3% ethylidene-norborene. EPDM used in the present work was reinforced with ceramic particles of

Bayerite (alumina-trihydrate, ATH) in a proportion of 44 wt%, as it is usual for electrical applications in order to improve the flashover resistance [1].

3.2 NEUTRON IRRADIATION

Neutron irradiations were performed at the RA-6 nuclear reactor of the National Atomic Energy Commission of Argentina. The RA-6 was operated at 400 kW. All samples were irradiated with bismuth and cadmium filters at room temperature in air. The thermal and fast neutron fluxes were $1.7x10^8$ n/cm²s and $5.5x10^8$ n/cm²s, respectively. The doses for the used samples were 82, 415, 830, 4150 and 8300 Gy. Dummy specimens of EPDM, which were irradiated together with the samples were studied by means of IR in order to check if oxidation was promoted during the neutron irradiation. IR studies could not reveal the appearance of oxidation in all the irradiated samples.

3.3 MEASUREMENTS

Positron lifetime measurements were performed at 300 K by a conventional fast–fast timing coincidence system with a resolution (full width at half maximum) of 240 ps. As positron source a ^{22}NaCl source of about 15 μCi evaporated onto a thin Kapton foil was used. The measuring time of all the neutron irradiated samples was similar. All lifetime spectra were analyzed in three components after subtracting the source contribution. The LT_92_3 program [23] to fit the spectra with a continuous distribution of positron lifetimes for the long lifetime τ_3 was used. In the present work we are interested in the evolution of the average of the free volume; so, we have particularly analyzed the parameters of the long component, lifetime and intensity, which are related to the free volume present in the sample. Indeed, following the common interpretation of PALS measurements in polymers, the long-lifetime component (τ_3) is associated with ortho-Ps annihilation by pick-off processes. From that, the mean size of the holes forming the free volume can be roughly estimated by means of the Eldrup model [24]. In such a model, the ortho-Ps lifetime, τ_3, as a function of the free-volume radius, R, is given by,

$$\tau_3 = 0.5 \left[1 - \frac{R}{R_0} + \frac{1}{2\pi} \sin \left(\frac{2\pi R}{R_0} \right) \right]^{-1} \quad (9)$$

where, $R_0 = R + \Delta R$ and τ_3 is given in nanoseconds. The radius ΔR is an empirical parameter whose best-value obtained fitting all known data is 1.656 Å [25]. The mean free volume hole size, V_f, assuming a spherical form for the holes, may be estimated by means of the following equation:

$$V_f = \left(\frac{4\pi}{3} \right) R^3 \quad (10)$$

The experimental data of a positron lifetime experiment in polymers are usually the convolution of three exponentials decays (i.e. three different lifetimes) with the resolution function of the spectrometer. Each lifetime corresponds to the inverse of the average annihilation rate of a positron in that state: the shortest and the intermediate lifetimes have contributions from the singlet para-positronium ($\tau_1 \approx 0.12$ ns) and positron annihilation in different molecule species; on the other hand, the longest lifetime ($\tau_3 \geq 1$ ns) is due to ortho-Ps localized in free volume holes. In this analysis, the τ_3 component is used to determine the mean free-volume hole size. The relative intensity corresponding to this lifetime, I_3, contains information related to the number of the free-volume holes from which positronium annihilates. In this sense, combining the number (I_3) and size (τ_3) of free volume holes an estimation of the free volume fraction (f) could be extracted [26]:

$$f = A V_f \, I_3 \quad (11)$$

where A is a proportionality constant, which can be determined by calibrating with other physical parameters [27, 28]. However, it is difficult to know the value of A for many polymers. So, Li et. al. have defined an apparent fractional free volume (AFFV) by the following equation [29]:

$$f_{app} = V_f \, I_3 \quad (12)$$

Dielectric strength, DS, measurements were performed immersing the EPDM samples into a dehydrated soybean oil bath thermalized at (300.0 ± 0.3) K and (323.0 ± 0.3) K. The cell for the bath is cubic with a volume of 350 cm^3 and it was constructed in atactic poly-methyl methacrylate (PMMA). Oil was dehydrated at 358 K during 24 hours, since the highest value of dielectric strength was achieved after such period of time [30]. Dehydrated soybean was used as oil bath due to the higher dielectric strength than mineral oil (YPF64) used in oil bath transformers employed for distribution.

EPDM samples for dielectric strength tests were parallelepiped shaped samples of 15 mm x 15 mm x 4 mm. Dimensions were determined with an error of around 0.02 mm. Electrodes were cylinders of stainless steel with 2 mm diameter, with flat base. Samples were placed between the two electrodes, with a gap of 4 mm, which were in soft contact with the surface of the sample. A schematic representation of the experimental set-up is shown in Figure 2.

The equipment for measuring DS, has an automatic rising voltage at 2 kV/s. It also has an automatic detection system for the cut of the run-up in voltage by measuring the derivative of the current increase. The voltage and current behaviors in the primary coil of the transformer were also monitored.

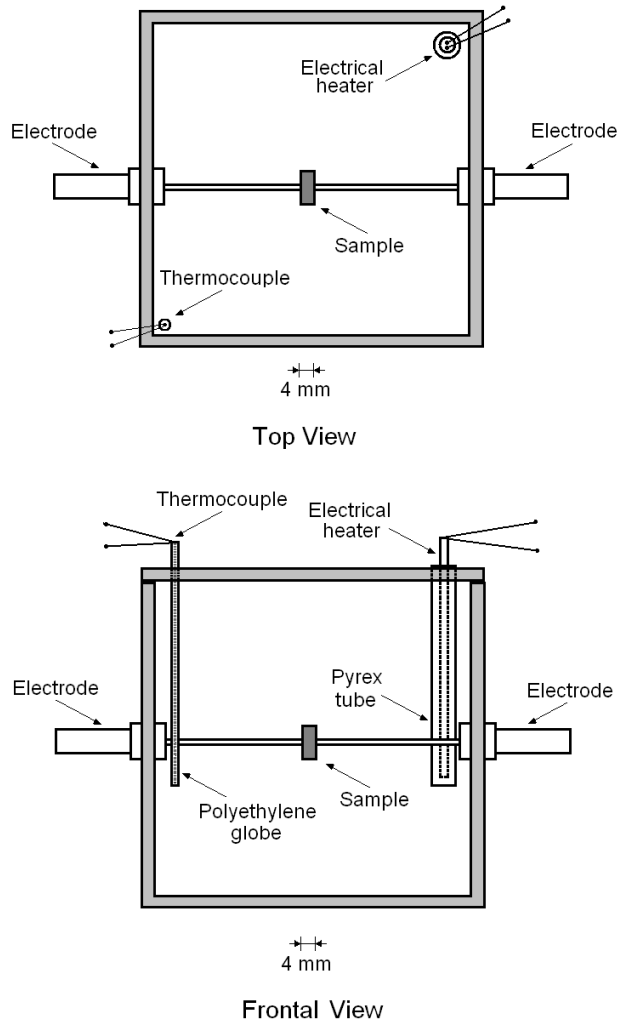

Figure 2. Thermalized oil bath cell for dielectric strength measurements.

Prior to DS measurements, the surfaces of the sample were carefully cleaned and washed in bidistilled water and subsequently dried in air at 300 K during 12 hours. If the cleaning of the sample is avoided arcs may appear on the surface of the sample.

The values of the voltage required for breaking the dehydrated soybean oil with a gap between the cylindrical electrodes of 4 mm at 300 K and 323 K were (68 ± 2) kV and (62 ± 2) kV.

Plotted values of DS in Figure 6 are the result of 8 measurements performed in two different samples, four measurements by sample. In each sample four positions for locating the electrodes were chosen in order to describe one square of 5 mm edge. The positioning of the sample into the cell was done by means of a magnifying glass and plastic tweezers. After introducing the sample, the oil bath is stirred in order to facilitate the thermal equilibrium. The measurement begins after the temperature is stable.

By means of a magnifying glass, it was verified that the arcs were through the sample. Figure 3 shows a typical puncture obtained from the DS tests. Color changes are observed in concentric circles on the damaged area. These, can be related to chemical changes in the polymer chains during the rupture process.

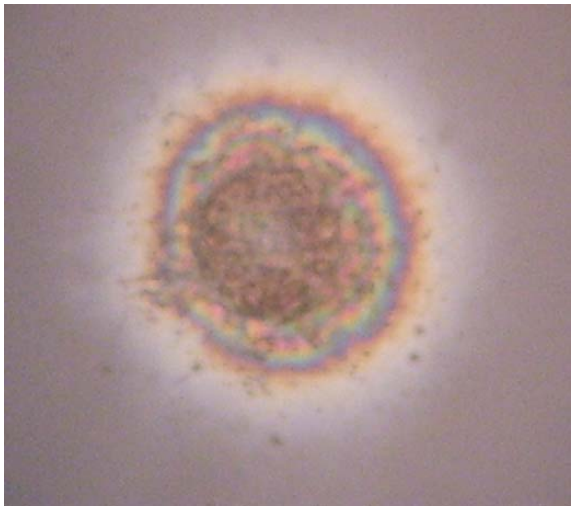

Figure 3. Typical puncture (X200) obtained in our equipment for EPDM samples recorded at 300 K. Photo corresponds to a sample irradiated at 830 Gy.

After four measurements the sample was retired from the cell and the stability of the breakdown voltage for the soybean oil was checked. No changes in the breakdown voltage for the oil during and after finishing the measurements were found. All the first measurements of DS were eliminated from the statistics, as it is usual for this test.

Measurements of dynamic mechanical analysis, DMA, loss tangent (damping or internal friction), tan(ϕ), and dynamic shear modulus, G', were carried out as a function of temperature at frequencies close to 5 Hz. Measurements were performed during heating with a heating rate of 1K/min. The temperature range of the measurements was between 180 K and 380 K. Measurements were performed under Argon atmosphere at atmospheric pressure. The samples for DMA studies were parallelepiped bars of around 5 mm width, 4 mm thick and 30 mm length. The maximum shear strain on the sample was $2x10^{-4}$. tan(ϕ) values were independent of the amplitude of the oscillating strain, i. e. doubling the applied stress led to the doubling of the strain response [31]. The estimated uncertainties for tan(ϕ) and G' were less than 3% and 10%, respectively.

Differential Thermal Analysis, DTA, measurements were performed in a conventional calorimetric equipment employing stainless steels crucibles under argon at atmospheric pressure. The employed heating rates were 5, 10 and 15 K/min, starting from liquid nitrogen temperatures.

X-rays diffraction, XRD, measurements were carried out employing a X-Pert Phillips 5000 powder diffractometer

working in reflection mode at room temperature. The Cu ($K\alpha_1$) wavelength (λ = 1.540562 Å), with monochromator, was used as incident radiation. The measurement conditions were: acceleration voltage: 40 kV, filament current: 20 mA, step in 2θ: 0.02° and the counting times were: 5 and 50 seconds (in each 2θ step).

4 RESULTS AND DISCUSSION

Figure 4 shows the behavior of the hole free volume (V_f), and the apparent fractional free volume, AFFV (V_f x I_3), determined from PALS (see Section 3.3) for the non-irradiated and irradiated samples as a function of irradiation dose. As it can be seen from the Figure, the AFFV increases monotonously as the irradiation dose increases, since the increase in the volume fraction of the crystalline zones, promoted by neutron impacts through a chemicrystallization process. In fact, neutron irradiation produces chain scissions, the scission products having less restricted mobility. Disentanglement of such fragments allows them to crystallize into imperfect, low-melting point crystals, increasing the overall crystalline content [16, 17, 32-35]. Chemicrystallization is produced by the piling up of nearby located cut polymer chains of the amorphous matrix. The length of the polymer chains per unit area, within the newly formed crystalline zone, is shorter than when the same zone is amorphous, leading to a less dense matrix. Therefore, the AFFV (empty space) increases with the increase in the volume fraction of the new crystallites [18].

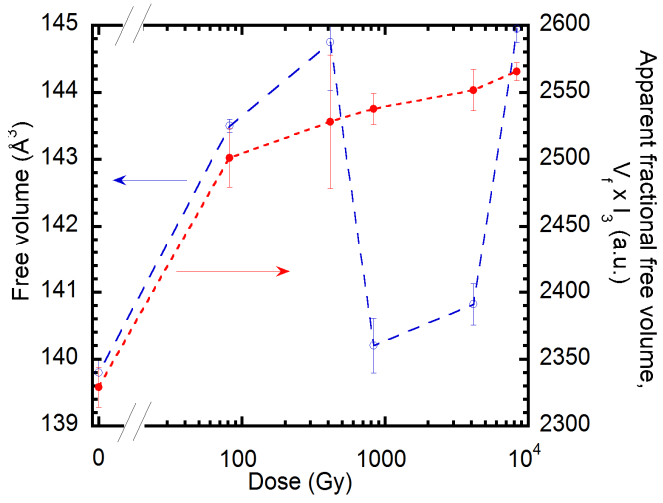

Figure 4. Free volume (empty circles) and apparent fractional free volume, V_f x I_3, (full circles), determined from PALS at room temperature, for non-irradiated and irradiated samples. Dashed lines are a guide for the eyes.

Figure 5 shows, two very simplified 2D views of the semi-crystalline rubber, accordingly to the stages controlled by irradiation. In this Figure the influence of the developed chemicrystallization on the total length of the chains per unit of area can be observed [4, 18].

The behavior of the hole free-volume as a function of the irradiation dose is also shown in Figure 4. As the free volume from PALS measures the size of the holes into the polymer matrix we can deduce the following evolution according to dose: The size of hole increases up to an irradiation dose of 415 Gy, and it decreases to a value close to the non-irradiated sample for an irradiation dose of 830 Gy. Subsequently, for higher irradiation doses the free volume increases again, reaching its highest value for a dose of 8300 Gy. In fact, recently, it was reported that the size of the holes into the polymer matrix is controlled by the size of the crystals. A larger size of the crystals leads to larger size in the hole free volume and vice-versa [18, 19]. This correspondence is explained by means of the inclusion theory, when the inclusion is smaller than the size of the hole into the matrix as it was shown in Section 2. In addition, this enlargement of the crystal size caused by the process of chemicrystallization during irradiation was explained as related to the decrease of the energy in the small inclusions/matrix interface, with crystal growth [17].

Figure 6 shows, by means of squares, the behavior of the dielectric strength, DS, measured at 300 K for non-irradiated and irradiated samples. As it can be seen from the Figure, the values of DS decrease as the dose increases. Moreover, it is interesting to note that a marked step-down at 830 Gy happens. We will return to this behavior in the following paragraphs.

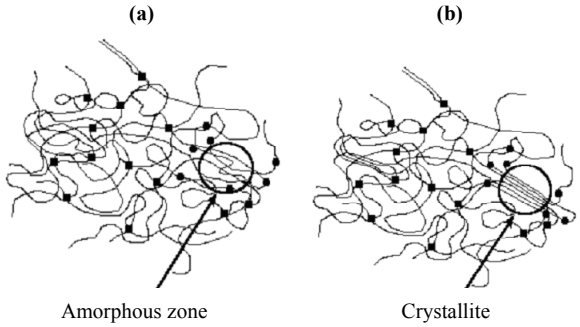

Figure 5. Very simplified 2D views of the semi-crystalline rubber, accordingly to the stages controlled by irradiation, from where the differences in the total length of the chains can be observed. (a) Prior to irradiation: an amorphous zone exists. (b) After irradiation: a crystalline zone develops by means of chemicrystallization.

The good correspondence between the behavior of the AFFV (Figure 4) and DS measured at 300 K (Figure 6), as a function of the irradiation dose should be highlighted. We are relating AFFV with DS curve measured at 300 K, since PALS is performed at this temperature. As it can be observed in Figure 7, an increase in AFFV leads to a decrease in DS. The decrease in DS as the empty space (AFFV) in the sample increases can be easily understood, taking into account the mobility of the polymer chains inside the polymer matrix. In fact, a larger quantity of empty space gives more room to accommodate the displacement and/or bend of the polymer chains for starting their movement, leading finally to the

massive movement of the polymer chains. This mechanism is in agreement with the relation, which is hold by the empty space (AFFV) and the activation energy for the movement of the polymer chains into a polymer [36]. By considering the polymer chain as a dislocation line and by taking into account the dislocation theory in continuous media, the larger quantity in empty space gives rise to a smaller energy saddle point to overcome the movement. Then, the movement of the chains becomes easier and consequently the DS value decreases. Indeed, charges come from the curing process of the rubber, electric carriers injected from the electrodes, ions from the corona effect, etc.. The ones placed inside or adjacent to the polymer chains have a mobility, for sweeping distances at mesoscopic scale, that is strongly dependent on the mobility of those polymer chains. In other words, a charge inside a space or micro-space, inside the entanglement of the polymer chains, under the application of an external electric field, will produce and electrical force on the polymer chains. The movement of this charge through a mesoscopic distance depends on the movement of the involved polymer chains. In addition, charges which exist after the curing process in the molecular chains were reported to operate as actuators in EPDM for destroying the crystallinity due to the shaking of the crystals under the effect of the electrical field in service [4]. Moreover, the appearance of cavities as hostage for charges, after damage of the polymer structure by fatigue mechanisms, was also reported in the literature [13, 37]. In this work the movement of the polymer chains is proposed as the mechanism, which controls the mobility of charges within the polymer matrix at mesoscopic scale.

In fact, the movement of the polymer chains are always involved in the electrical breakdown phenomena, even if the subject under study is for instance: (a) the behavior of the initial branches of treeing formed by the action of partial discharges between the needle tip and the ends of the branches [13], (b) the combined effect of the thermal wave produced by the discharge and the propagation of the branches for the breakdown of the material, and (c) the injection of charges from the electrode [5, 13, 37-41]. Then, the movement of the charges embedded in the chain entanglement, over distances at mesoscopic level is always dependent on the mobility degree of the entanglement of the polymer chains in the matrix, as it could be expected.

Besides, the relation of the polymer chains to dislocation lines arises after the study of the viscoelastic behavior of polymers in earlier times [42, 43]. Molecular chains are considered in movement trying to overcome a potential energy barrier. When the applied force on the molecular chain is zero, the jump frequency is given by the usual Arrhenius law [44]. In contrast when the stress is acting on the molecular chain, a non symmetric jump develops and the simple Arrhenius dependence for the jump frequency splits into two laws depending on the jump direction. These expressions are very similar to the ones proposed for the dislocation line in movement in metals, when the dislocation is studied in a continuous media [45, 46].

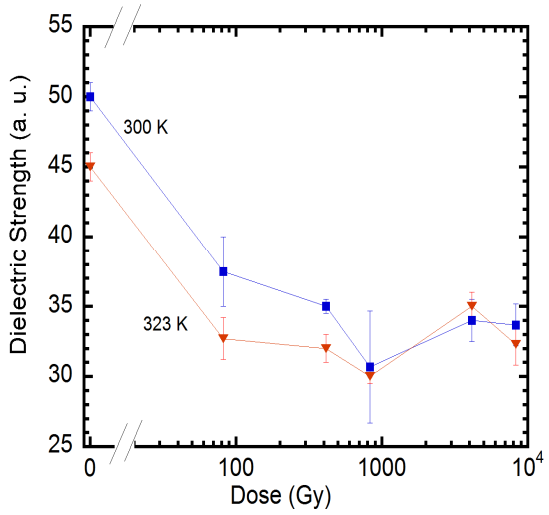

Figure 6. Dielectric strength in arbitrary units measured in non-irradiated and irradiated EPDM samples. Squares: Samples measured at 300 K. Inverted triangles: Samples measured at 323 K.

On the other hand, the experimental data in Figure 7 can be very well fitted by a square polynomial. However, the value at 830 Gy, moves aside from the behavior of the other points. If we remove this value, corresponding to a dose of 830 Gy, the correlation factor of the fitting to a square polynomial of the experimental data, increases appreciably; r = 0.9987.

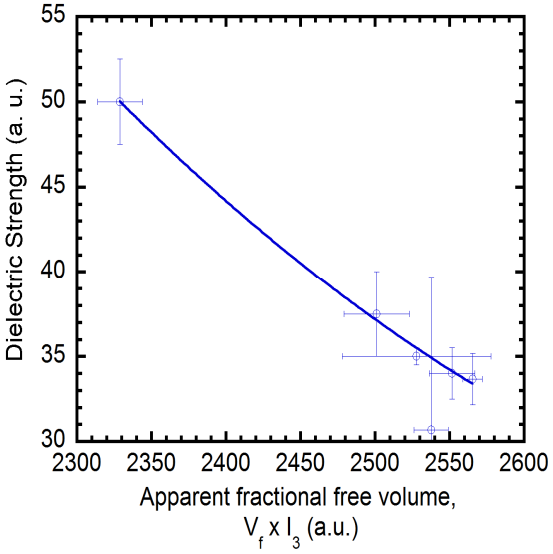

Figure 7. Dielectric strength as a function of the AFFV. In the fitted curve the point at 830 Gy is not included, see explanation in the text.

Attention must be paid at this dose, in both, the DS (see Figure 6) and the free volume (see Figure 4) decrease. The behavior exhibited by the free volume, suggests that some change in the internal stresses into the polymer matrix develops at this dose. Then in order to study the internal stresses in EPDM samples, we have performed DMA measurements and we have calculated the values of the β coefficient (see Section 2) as a function of the irradiation dose.

Figure 8 shows tan(ϕ) spectra for non-irradiated and irradiated samples in the temperature range 260-380 K. For each spectrum only one of every three measured points was plotted for clarity. As it can be seen from the Figure, tan(ϕ) values increase as the irradiation dose increases, developing a peaked-shape spectra, which is related to the melting of the crystalline zones in EPDM [4, 16-20, 33-35]. In addition, the increase in the values of tan(ϕ) maximum, within 280 K and 380 K, was related in previous works to the increase in the volume fraction of crystallites promoted by neutron impacts through a chemicrystallization process.

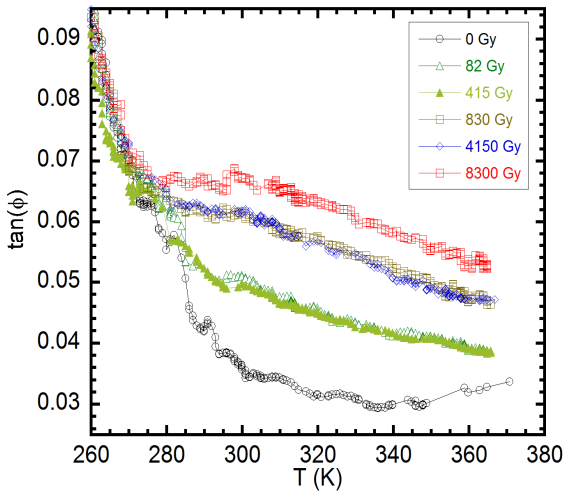

Figure 8. tan(ϕ) spectra for the non-irradiated and irradiated samples measured during the first heating.

The dynamic shear modulus as a function of temperature for the spectra plotted in Figure 8 is shown in Figure 9. We have modified slightly the temperature range for the moduli curves in order to facilitate the observation of the behavior of each curve, within the temperature range of interest for this work. As it can be seen from the Figure, the development of crystalline zones, promoted by neutron impacts, leads to an increase of the dynamic modulus. However, the sample irradiated at 830 Gy exhibits smaller values of G' than the samples irradiated at 415 Gy and at 4150 Gy. Sample irradiated at 8300 Gy shows the smallest values of G', among irradiated samples, due to the destruction of the polymer matrix promoted by neutron impacts at the highest dose used in this work [17-19].

DMA results give also additional information, which is briefly summarized below. tan(ϕ) spectra for temperatures smaller than around 290 K also show the high temperature tail of the relaxation related to the glass transition, Tg. No changes in Tg as a function of the irradiation dose were found. The value for Tg was around 240 K for all the EPDM studied samples.

Besides, the temperature where the maximum in tan(ϕ) appears is related to the size of the crystalline zones which are melting. In fact, the bigger the size of the crystalline zones, the higher the temperature of the maximum for tan(ϕ) [16-19, 34, 35]. However, in these spectra, a clear variation of the temperature where the maximum appears cannot be established. Depending on the crystalline arrangement, sometimes the temperature for the maximum cannot be determined clearly [16-18].

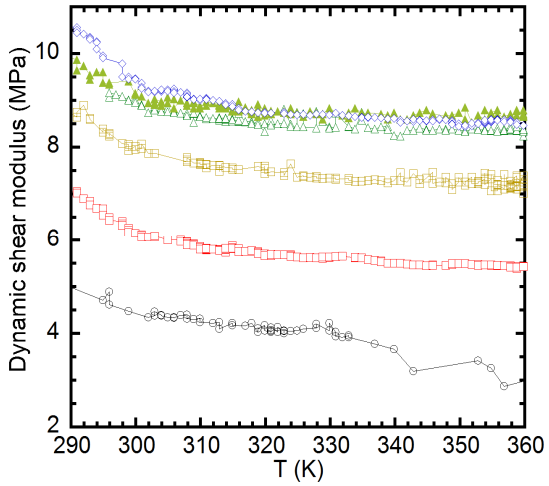

Figure 9. Dynamic shear modulus as a function of temperature for the spectra plotted in Figure 8. The symbols are identical to the ones in Figure 8.

It is convenient to comment here, that the connection of the tan(ϕ) maximum with the melting of the crystalline zones in EPDM was also verified by means of dielectric relaxation (DR) and PALS studies in previous works [19, 20, 47]. Our results are also in agreement with previous reported works by other authors [32, 48]. In addition, it has been also demonstrated in previous works that this tan(ϕ) maximum, has no contribution of an interaction process at the interfaces between the filler and the rubber [4]. In fact, it should be highlighted that in the present work tan(ϕ) values were amplitude independent (see Section 3.3) [4, 31]. The amplitude independent behavior in tan(ϕ), within the whole temperature range of the DMA measurements, was also corroborated in dummy samples, which were measured up to a maximum shear strain on the surface of 1%. Also samples deformed 100% were checked as in [4], corroborating the amplitude independent behavior in tan(ϕ). Therefore, dissipative contributions from the zone at the interface filler/rubber can be rejected in the studied samples of the present work.

In order to calculate the β coefficient for the non-irradiated and irradiated samples (equation (7) in Section 2), the values obtained from four different DMA tests in different samples of the same type were used.

Figure 10 shows the behavior of the β coefficient as a function of the irradiation dose for the studied samples. Plotted values are the mean value obtained in the tests and the error bars correspond to the largest scatter between the

calculated points. Figure 10 shows that β decreases as the irradiation dose increases, with exception of the data calculated for the sample irradiated at 830 Gy. The decrease in β as the irradiation dose increases can be related to the increase in the internal stresses promoted by the growing of the crystals by neutron irradiation, as it was already mentioned (see Section 2), in agreement with previous works [18, 19]. In contrast, the increase of β at 830 Gy indicates the decrease in the internal stresses at this dose, which is in agreement with the decrease in the free volume, see Figure 4.

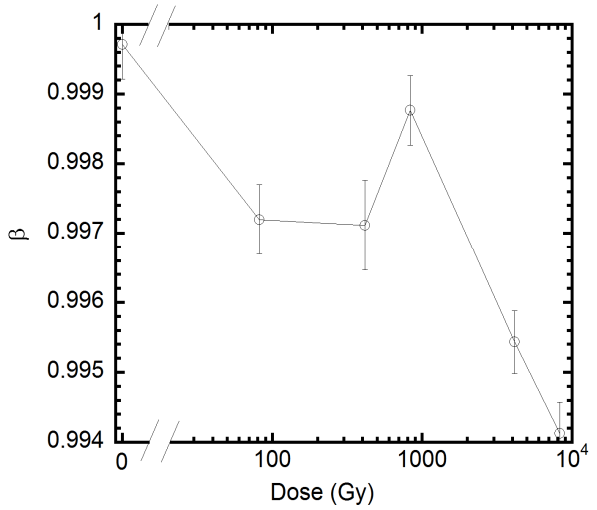

Figure 10. Behavior of β coefficient as a function of the irradiation dose.

It should be remarked that the decrease of the internal stresses, which occurs at 830 Gy is accompanied by an increase of the empty space (AFFV) in around 10%, with respect to the non-irradiated sample (see Figure 4). Then, it allows local movements of the polymer chains, which can be promoted by applying an electrical force, since the line tension of the polymer chain has decreased. Indeed, in DS test, the decrease of the internal stresses, when the empty space has increased, allows the arising of preferable places for the bend of isolated polymer chains in local zones. It should be pointed out that, these bends are the precursors for the subsequent development of the electrical breakdown, since charges can now start the movement, at mesoscopic scale. Consequently, DS is also very sensitive to the change in the internal stresses acting at the polymer chains, even if these changes cannot be so clearly resolved in the DS versus AFFV plots. Therefore, DS depends on the empty space into the polymer matrix (AFFV) and also on the internal stresses arrangement acting at the polymer chains.

In order to check the contribution of the internal stresses into the polymer as a beneficial element for increasing DS, we have also performed DS measurements at 323 K for non-irradiated and irradiated samples, see inverted triangles in Figure 6. DS measured at 323 K, decreases as the dose increases, being the values of DS measured at 323 K smaller than the measured ones at 300 K, up to 415 Gy. In contrast, for higher doses it should be remarked that both DS curves overlap. Moreover, for the two DS curves, it is interesting to note that a marked step-down at 830 Gy happens.

Besides, we have derived from the formalism presented in Section 2, the expression for the internal stresses in the amorphous phase of the polymer. From the Reuss approximation to the equilibrium of mechanical stresses between the inclusion and the matrix [21] and working mathematically, we can easily obtain the internal stresses of the amorphous matrix, *Tm*, as a consequence of the appearance of the new crystals, such that

$$\frac{Tm}{\in} = E_{\mathrm{m}}\ \beta^{z}\ \left(\frac{fr_i^{z}}{fr_m^{z}}\right) \tag{13}$$

For simplicity we have obtained the ratio between *Tm* and the misfit parameter ∈ since this last is unknown. As it was introduced in Section 2, ∈ is the mismatch parameter between the size of the hole and the size of the inclusion. In the next paragraphs we will demonstrate that the variation of ∈ between the different samples used in this work can be neglected.

Then, the values of $Tm/\in$ for different temperatures, using β (equation (7)), and E_{m} and fr_i as a function of temperature from the DMA data, can be obtained. It is convenient to mention that the expressions for the calculus of β and $Tm / \in$ invoke the values of Young moduli, however we have used instead the dynamic shear modulus in the present calculations, as it was already done in previous works [19, 20]. This does not represent a problem, because of the mean field approximation used in the model developed in Section 2; consequently it does not diminish the present results and the subsequent analysis.

Here, the behaviour of $Tm / \in$ is shown instead of that of β, because its variation as a function of the temperature is two order of magnitude higher than the variation of β. In addition, *Tm* was calculated for the amorphous phase, because in EPDM it is the major phase in comparison to the crystalline one, as it is revealed by the DTA and X-rays results, which are show in the next paragraphs. In fact, EPDM chains are composed by a random arrangement of ethylene, propylene and diene monomers. In contrast, the crystallites are composed by chains having predominantly long sequences of ethylene groups.

Figure 11 shows the behavior of the internal stresses at different temperatures, for three samples irradiated with different doses. The large decrease in $Tm / \in$ for the different temperatures confirms that the distortion introduced to the value of *Tm* due to changes in ∈ as a consequence of the change in temperature, is negligible. If the variation in ∈ would be significant, the ratio $Tm / \in$ would increase as a function of temperature, but it is not the case.

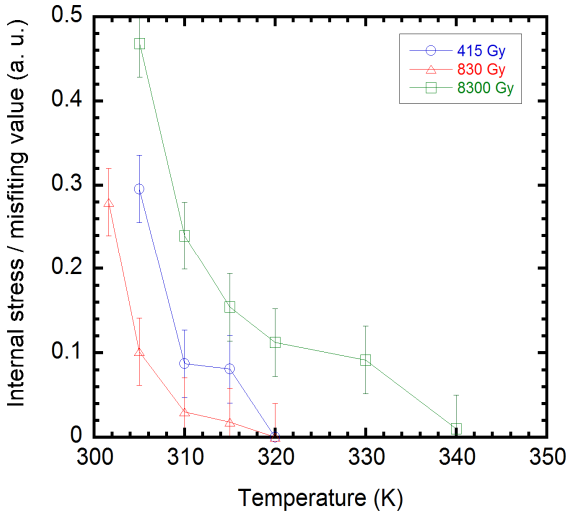

Figure 11. Ratio between the internal stresses of the amorphous matrix, *Tm*, as a consequence of the appearance of the new crystals, and the misfit parameter ∈; *Tm* / ∈, equation (13), for different temperatures and for three different irradiation doses.

As it can be seen from Figure 11, the internal stresses decrease as the temperature becomes higher than the temperature where the maximum in tan(ϕ) appears (see Figure 8). Curve for samples irradiated at 82 Gy and 4150 Gy behave completely similar to the curves corresponding to 415 Gy and 8300 Gy, respectively; but they were not shown for clarity. At temperatures over the maximum in tan(ϕ) only the larger crystals remain, since the smaller ones have melted. The melting decreases the volume fraction of the crystals giving rise to the release in the internal stresses into the polymer matrix.

Only samples with the largest volume fraction of crystals (samples irradiated at 4150 Gy, not shown in the Figure, and 8300 Gy, see Figures 4 and 8) exhibit still the appearance of internal stresses for temperatures over 320 K. However, sample irradiated at 830 Gy, releases the internal stresses at 320 K. This sample, in addition, exhibits the smallest values of the internal stresses as a function of temperature, which is in agreement with the behaviour of both, the value of its free volume and its β value. See Figures 4 and 10, where these values are shown as function of the irradiation dose.

The state of the internal stresses in each studied sample depending on the crystalline state have been now determined. Then, let's return to the discussion of the behaviour of DS with temperature. When DS is measured at 300 K, the sample has internal stresses, due to the development of the crystalline zone by the chemicrystallization process. From that point on, the electrical force, which is pushing the polymer chains, in order to start their bend, has firstly to overcome the chain line tension, related to the internal stresses. Subsequently, for starting the movement of the polymer chains, the electrical force must overcome the average energy saddle point of the chains arrangement, which is related to the apparent fractional free volume (AFFV).

In contrast, when DS is measured at 323 K, in samples irradiated up to 830 Gy, the experiment is carried out at a temperature higher than the one which corresponds to the maximum in tan(ϕ), see Figure 8. In this case most of the crystals have melted, i.e. the volume fraction of crystals has decreased markedly; leading to the decrease in the internal stresses, see Figure 11. It can be said that for these irradiations up to 830 Gy the internal stresses are almost nil. Then the electric force required for starting the local movement of the polymer chains has decreased, leading to appreciably lower values in DS for 323 K than for 300 K. Only samples with both, larger volume fraction and larger internal stresses acting at the polymer chains, that is, samples irradiated at 4150 Gy and 8300 Gy, will have enough quantity of crystals at 323 K, in order to take enough tensile internal stresses for resisting the electrical forces. Therefore, for these samples, the internal stresses appearing by the crystalline state promoted by chemicrystallization, oppose to the electrical force and they are strong enough for compensating the thermal vibrational energy of performing the DS test at 323 K. This leads to similar DS values for these irradiation doses (4150 Gy and 8300 Gy) measured at 300 K and 323 K. Therefore, it can be proposed that in this case the precursor for the electrical breakdown is the local bend of the polymer chains promoted by the electrical forces.

On the other hand, DTA thermograms for all irradiated and non-irradiated samples, exhibited a wide endothermic reaction within around 280–350 K, related to the melting of the crystalline zones. Figure 12 shows the thermograms measured, at 5K/min, for non-irradiated and 8300 Gy irradiated samples after the base line subtraction. Plotted curves correspond to samples where the largest difference was found. Thermograms for another samples used in this work are within these two spectra.

In addition, from the DTA tests performed at different heating rates (see Section 3.3), clear changes between the thermograms recorded in the different samples could not be detected. The lack of resolution in the thermograms can be related to the small mass involved by the crystals in contrast to the whole mass of the sample.

Figure 13, shows the X-rays diffraction patterns for a non-irradiated and 8300 Gy irradiated samples. Patterns measured for all the irradiated and non-irradiated samples showed a wide reflection peak at around 2θ = 18°, which could be related to the crystalline zones, together with overlapped reflections corresponding to the triclinic lattice of the Bayerite (alumina-trihydrate, ATH). Semi-crystalline polymer structures are characterized by a lack of periodicity and small zones with tendency to order in the sense that the atoms are tightly together and show a statistical preference for a particular interatomic distance. The result is an X-ray scattering pattern showing one or two broad maxima in the region of 2θ smaller than around 25° [49].

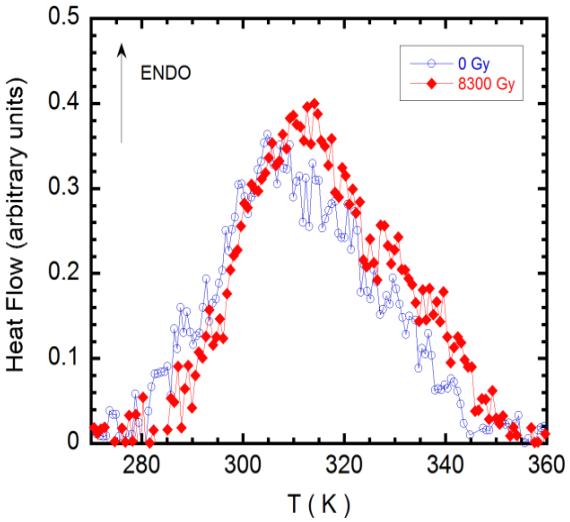

Figure 12. DTA thermograms for non-irradiated and 8300 Gy irradiated samples after the subtraction of the base line.

Nevertheless, clear changes in the integrated intensity of the reflection peak related to the crystals could not be observed, even if the samples were measured using the longest counting time.

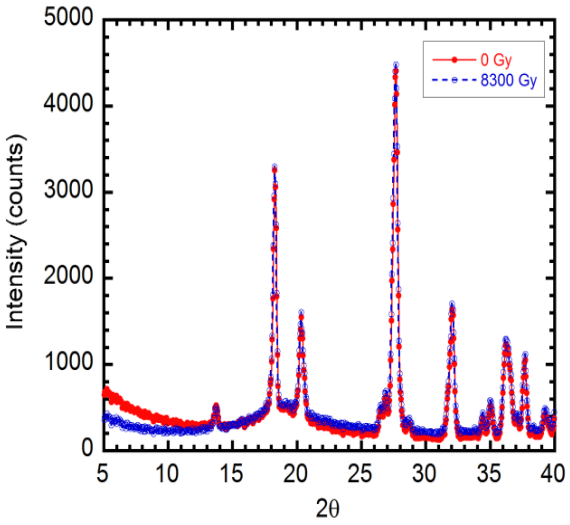

Figure 13. X-ray (Cu, $K\alpha_1$) diffraction patterns for a non-irradiated and 8300 Gy irradiated sample measured at room temperature.

This lack of discrimination for the XRD measurements is in agreement with the level of resolution of the XRD technique, which depends on the volume fraction and morphology involved. In fact, the intensity of the diffracted beam depends on many factors. One of them is the scattering factor, which describes interference processes between the atoms and the wavelength of the incident radiation. In addition, the intensity of the diffracted beam depends also on the type and quantity of atoms producing diffraction, the so called structure factor. Then a large quantity of diffracting elements leads to more intense diffraction peaks [49, 50]. Indeed, X-ray diffraction studies have a resolution limit of about 1-3% of the volume fraction of the second phase. Consequently, we can conclude that the range of diffraction angles employed in XRD studies with Cu ($K\alpha$) radiation in this work is not appropriate for detecting these crystals. Indeed, it could be necessary to work at small angles in diffraction studies using X-rays or neutrons [49, 51].

It should be remarked that the limitations in the resolution of XRD and DTA techniques, found in this work for studying the change in the crystalline degree promoted by chemicrystallization process in EPDM, are in agreement with previously reported works in the literature [33, 52, 53].

5 CONCLUSIONS

The dependence of DS on both, the empty space into the sample and the internal stresses acting at the polymer chains, which result from the crystalline state promoted by chemicrystallization, was determined. Both phenomena are acting overlapped and in competition against the electrical force working on the polymer chain.

When crystalline zones are promoted into the matrix in semi-crystalline EPDM and the internal stresses increase, DS decreases as the empty space (AFFV) into the sample increases, owing to the movement of the polymer chains. This movement is mainly controlled by the empty space into the sample, since the entanglement of chains leads to a collective movement of them where no preferable and isolated bends occur. However, when the internal stresses acting at the polymer chains decrease, there appear local zones where the polymer chains start the bend, once the electrical forces are larger than the line tension.

Consequently, this effect elucidates that the bends of preferable sites are the precursor for the collective movement of polymer chains leading to the electrical breakdown phenomenon. Smaller internal stresses, lead to smaller line tensions at the polymer chains, which lead to smaller DS values.

ACKNOWLEDGMENT

This work was partially supported by the Collaboration Agreement between the Universidad del País Vasco and the Universidad Nacional de Rosario Res. 1792/2003, UPV224.310-14553/02, Res. 3469/2007 and Res. 124/2010, the CONICET-PIP No. 2098, the PID (ING 288) 2010–2013 and the Collaboration Agreement between PETROBRAS ENERGÍA S. A., Puerto General San Martín, Pcia. de Santa Fe and the Instituto de Física Rosario (IFIR) – CONICET, 2008-2012. We are also indebt to Eusko Jaurlaritza for the support under Grant No. IT-443-10.

REFERENCES

[1] R. Hackam, "Outdoor HV Composite Polymeric Insulators", IEEE Trans. Dielec. Electr. Insul., Vol. 6, No. 5, pp. 557-585, 1999.

[2] J. T. Burnham and R. J. Waidelich, "Gunshot Damage to Ceramic and Nonceramic Insulators", IEEE Trans. Power Delivery, Vol. 12, No. 4, pp. 1651-1656, 1997.

[3] W. W. Pendleton, (Chapter Editor) *Encyclopedia of Materials Science and Engineering*, M.B. Bever (Editor), Vol. 2, Pergamon Press: Oxford, 1986.

[4] P. A. Sorichetti, C. L. Matteo, O. A. Lambri, G. C. Manguzzi, L. M. Salvatierra, and O. Herrero, "Structural changes in EPDM subjected to ageing in High Voltage Transmission Lines", IEEE Trans. Dielec. Electr. Insul., Vol. 14, pp. 1170 – 1182, 2007.

[5] J. Ulanski and M. Kryszewski, "Polymers, Electrical and Electronic Properties", in *Encyclopedia of Applied Physics*, Ed. Trigg G. VCH Publishers, Inc., New York, Vol. 14, p. 497, 1996.

[6] S. Kumagai, *Fundamental Research on Polymeric Materials Used in Outdoor High Voltage Insulation*, Ph.D. thesis, Akita University, Japan, 2000.

[7] J. P. Reynders, I. R. Jandrell, and S. M. Reynders, "Review of aging and recovery of silicone rubber insulation for outdoor use", IEEE Trans. Dielectr. Electr. Insul., Vol. 6, No. 5, pp. 620-631, October 1999.

[8] N. H. Malik, A. A. Al-Abdullah, A. A. Al-Arainy, and M. I. Qureshi, "Factors influencing electrical treeing in XLPE insulation", Euro. Trans. Electr. Power, Vol.16, pp. 205–218, 2006.

[9] D. Birtwhistle, P. D. Blackmore, A. Krivda, G. A. Cash, and G. A. George, "Monitoring the Condition of Insulator Shed Materials in Overhead Transmission Networks", IEEE Trans. Dielectr. Electr. Insul., Vol. 6, pp. 612- 619, 1999.

[10] A. J. Phillips, D. J. Childs, and H. M. Schneider, "Water Drop Corona Effects on Full-Scale 500 kV Non-Ceramic Insulators", IEEE Trans. Power Delivery, Vol. 14, pp. 258-265, 1999.

[11] J. Kuang and S.A. Boggs, "Thermal-electric field distribution around a defect in polyethylene", IEEE Trans. Power Delivery, Vol. 13, No.1, pp. 23 – 27, 1998.

[12] A. E. Vlastos and T. Sörqvist, "Field Experience of ageing and performance of polymeric composite insulators", Électra, Vol. 171, pp. 117-135, 1997.

[13] C. Mayoux, *Die Angewandte Makromolekulare Chemie*, Vol. 261/262, pp. 143-145, 1998.

[14] M. A. Handala and O. Lamrous, "Surface degradation of styrene acrylonitrile exposed to corona discharge", Euro. Trans. Electr. Power (in press). Published online in Wiley InterScience (DOI: 10.1002/etep.189).

[15] L. Niemeyer, L. Pietronero, and H. J. Wiesmann, "Fractal dimension of dielectric breakdown", Phys. Rev. Lett., Vol. 52, No.12, pp. 1033–1036, 1984.

[16] L. M. Salvatierra, O. A. Lambri, C. L. Matteo, P. A. Sorichetti, C. A. Celauro and R. E. Bolmaro, "Growing of crystalline zones in EPDM irradiated with a low neutron flux", Nucl. Instr. Meth. B, Vol. 225, pp. 297-304, 2004.

[17] O. A. Lambri, L. M. Salvatierra, F. A. Sánchez, C. L. Matteo, P. A. Sorichetti, and C. A. Celauro, "Crystal growth in EPDM by chemi-crystallisation as a function of the neutron irradiation dose and flux level", Nucl. Instr. Meth. B, Vol. 237, pp. 550-562, 2005.

[18] O. A. Lambri, F. Plazaola, E. Axpe, R. R. Mocellini, G. I. Zelada-Lambri, J. A. García, C. L. Matteo, and P. A. Sorichetti , "Modification of the mesoscopic structure in neutron irradiated EPDM viewed through positron annihilation spectroscopy and dynamic mechanical analysis", Nuclear Inst. Meth. B, pp. 269, 336 – 344, 2011.

[19] R. R. Mocellini, O. A. Lambri, C. L. Matteo, J. A. García, G. I. Zelada-Lambri, P. A. Sorichetti, F. Plazaola, A. Rodríguez-Garraza, and F. A. Sánchez, "Elastic misfit in two-phase polymer", Polymer, Vol. 50, pp. 4696 – 4705, 2009.

[20] R. R. Mocellini, O. A. Lambri, C. L. Matteo, and P. A. Sorichetti, "Dielectric Properties and Viscoelastic Response in Two-Phase Polymers", IEEE Trans. Dielec. Electr. Insul., Vol. 15, pp. 982–993, 2008.

[21] T. Mura, *Micromechanics of defects in solids*, Martinus Nijhoff Publishers: New York, 1987.

[22] ASTM Standard D3900-05a, "Rubber-Determination of Ethylene Units in Ethylene-Propylene Copolymers (EPM) and in Ethylene-Propylene-Diene Terpolymers (EPDM) by Infrared Spectrometry", ASTM International, West Conshohocken, PA, 2005, (DOI: 10.1520/D3900-05A).

[23] J. Kansy, "Microcomputer program for analysis of positron annihilation lifetime spectra", Nucl. Instr. and Meth. A, Vol. 374, p. 235, 1996.

[24] M. Eldrup, D. Lightbody and J.N. Sherwood, "The temperature dependence of positron lifetimes in solid pivalic acid", Chemical Physics, Vol. 63, pp. 51-58, 1981.

[25] H. Nakanishi, S.J. Wang and Y.C. Jean, S.C. Sharma (Eds.), *Positron Annihilation Studies of Fluids*, World Scientific, p. 292, Singapore, 1988.

[26] Y.Y. Wang, H. Nakanishi, Y.C. Jean and T.C. Sandreczki, "Positron annihilation in amine-cured epoxy polymers", J. Pol. Sci. B, Vol. 28, pp. 1431-1441, 1990.

[27] J. Liu, Q. Deng and Y. C. Jean, "Free-volume distributions of polystyrene probed by positron annihilation: comparison with free-volume theories", Macromolecules, Vol. 26, pp. 7149-7155, 1993.

[28] Y. C. Jean, "Free-volume mean sizes of polymers probed by positron annihilation spectroscopy: a correlation of results obtained by PAL and by ACAR methods", Nucl. Instr. Meth. B, Vol. 56-57, Part 1, pp. 615-617, 1991.

[29] H.L. Li, Y. Ujihira, A. Nanasawa and Y.C. Jean, "Estimation of free volume in polystyrene-polyphenylene ether blend probed by the positron annihilation lifetime technique", Polymer, Vol. 40, pp. 349-355, 1999.

[30] P. A. Sorichetti, G. I. Zelada-Lambri, O. A. Lambri, C. L. Matteo, L. O. Schujman, J. A. Cano, R. R. Mocellini, and O. Herrero, "Study of thermodynamic and dielectric response in vegetable oils","Estudio de la Respuesta Termodinámica y Dieléctrica en Aceites Vegetales", [Décimo Tercer Encuentro Regional Iberoamericano del CIGRE (Consejo Internacional de Grandes Redes Eléctricas), XIII ERIAC 2009, Parque Nacional Iguazú, Argentina, 24-28 Mayo 2009].

[31] O. A. Lambri, "A Review on the problem of measuring non-linear damping and the obtainment of intrinsic damping", Materials Instabilities, in: D. Walgraef, J. Martínez-Mardones, C.H.Wörner (Eds.), World Scientific Publishing Co. Pte. Ltd., pp.249, 2000.

[32] J. Davenas, I. Stevenson, N. Celette, G. Vigier, and L. David, "Influence of the molecular modification on the properties of EPDM elastomers underirradiation", Nucl. Instr. Meth. B., Vol. 208, pp. 461-465, 2003.

[33] M. Celina, K. T. Gillen, J. Wise, and R. L. Clough, "Anomalous Aging Phenomena in a Crosslinked Polyolefin Cable Insulation", Radiat. Phys. Chem., Vol. 48, p. 613, 1996.

[34] A. Charlesby*, Atomic radiation and polymers*, Pergamon Press, Oxford, 1960.

[35] A. Charlesby and L. Callaghan, "Crystallinity changes in irradiated polyethylenes", Phys. Chem. Solids, Vol. 4, pp. 306-314, 1958.

[36] M. Ponsard-Fillette, C. Barrés, and P. Cassagnau, Polymer, "Viscoelastic study of oil diffusion in molten PP and EPDM copolymer", Vol. 46, p. 10256, 2005.

[37] J. P. Crine, S. Pelissou, H. St.-Onge, J. Pierre, G. Kennedy, A. Houdayer, and P. Hinrichsen, "Elemental and ionic impurities in cable insulation and shields", Int'l. Conf. Polymer Insul. Mater. Power Cables, JICABLE 87 p. 206, 1987.

[38] D.W. Auckland, A.B. Borishade, and R. Cooper, "Photographic investigation of breakdown of composite insulation", Proc. IEEE, Vol. 124, p. 1263, 1977.

[39] M. Ieda and M. Nawata, "DC Treeing Breakdown Associated With Space Charge Formation in Polyethylene", IEEE TDEI, Vol. 12, No. 26, 1977.

[40] F. Noto, N. Yoshimura, and T Oota, "Tree Initiation in Polyethylene by Application of DC and Impulse Voltage", IEEE TDEI, Vol. 12, No. 26, 1977.

[41] Y. Saito, M. Fukuzawa, and H. Nakamura, "On the Mechanism of Tree Initiation", IEEE TDEI,Vol. Vol. 12, No. 31, 1977.

[42] H. Eyring, "Viscosity, Plasticity, and Diffusion as Examples of Absolute Reaction Rates", J. Chem. Phys., Vol. 4, No. 4, p. 283, 1936.

[43] S. Glasstone, K.J. Caidler and H. Eyring, *The Theory of the Rate Processes*, McGraw Hill, New York, 1941.

[44] P. G. Shewmon, *Diffusion in Solids*, McGraw-Hill, New York, 1963.

[45] J. Friedel, *Dislocations*, Pergamon Press, Oxford, UK, 1967.

[46] R. Schaller, G. Fantozi and G. Gremaud, *Mechanical Spectroscopy*, Trans. Tech. Publ. Ltd., Switzerland, 2001.

[47] R. R. Mocellini, G. I. Zelada-Lambri, O. A. Lambri, C. L. Matteo, and P. A. Sorichetti, "Electrorheological description of liquid and solid dielectrics applied to two-phase polymers: A study of EPDM", IEEE Trans. Dielec. Electr. Insul., Vol. 13, pp. 1358-1370, 2006.

[48] J. P. Runt and J. J. Fitzgerald, *Dielectric Spectroscopy of Polymeric Materials, Fundamentals and Applications*, American Chemical Society, Washington D.C., 1997.

[49] B. D. Cullity, *Elements of X-ray Diffraction*, Addison-Wesley Publishing Co., Reading, 1967.

[50] C. Kittel, *Introduction to Solid State Physics*, John Wiley & Sons, New York, 1971.

[51] J. Baruchel, J. L. Hodeau, M. S. Lehmann, J. R. Regnard, and C. Schlenker (Eds), *Neutron and Synchrotron Radiation for Condensed Matter Studies*, Vol. II., HERCULES, Springer-Verlag, Les Editions de Physique, Berlin,1994.

[52] G. Lachenal, I. Stevenson, and N. Celette, "Near-infrared transmittance spectroscopy for radiochemical ageing of EPDM", The Analyst, Vol. 126, p. 2201, 2001.

[52] G. Lachenal, I. Stevenson, and N. Celette, "Near-infrared transmittance spectroscopy for radiochemical ageing of EPDM", The Analyst, Vol. 126, p. 2201, 2001.
[53] G. Lachenal, I. Stevenson, "Applicability of Fourier transform near infrared spectroscopy and principal components analysis for studying elastomers after radiochemical ageing", Journal of Near Infrared Spectrosc., Vol. 10, p. 279, 2002

Osvaldo Agustín Lambri was born in Rosario, Argentina in 1963. He obtained the B.Sc. and M.Sc. (physics, 1989) degrees from the Rosario National University (UNR) and the Ph.D. degree in physics (1993, focussed on materials science) from the same University. Post-doctoral position at the Laboratory of Materials in the University of the Basque Country, Bilbao, Spain. Guest Scientists at the Institut für Werkstoffkunde und Werkstofftechnick, Clausthal University of Technology, Clausthal Zellerfeld, Germany and at the Faculty of Science and Technology of the University of the Basque Country, Basque Country, Spain. Dr. Lambri is a member of the National Council of Research Staff of Argentina (CONICET) at the Institute of Physics of Rosario (IFIR). Since 2002 he is head of the Laboratory of Materials (LEIM) at the Electrical Engineering School (EIE) of the Faculty of Science and Engineering (FCEIA) - IFIR of the UNR – CONICET and an Associate Professor of Electrical Materials at EIE, FCEIA, UNR. He also was leader of Research Projects at the Institute Laue Langevin - Grenoble, France. His current research areas include the mechanical properties and phase transitions of super-alloys and refractory metals and the mechanical and electrical properties of polymers**.**

Federico Tarditti was born in Rosario, Argentina in 1988. He got his degree as electrical engineer from Rosario National University (UNR) in 2012. Nowadays he has got a fellowship from the National Council of Research of Argentina (CONICET). He also has a Doctoral position at the Laboratory of Materials (LEIM-IFIR-CONICET) at the Electrical Engineering School (EIE) of the Faculty of Science and Engineering (FCEIA) of the UNR. He is focused on the study of the relation of mechanical and electrical properties of polymer materials used in Electrical Industry.

José Ángel Cano was born in Rosario, Argentina in 1965. He obtained the electrical engineering degree from the Faculty of Science and Engineering (FCEIA) of the Rosario National University (UNR) in 1999 and the Ph.D. degree in engineering (focused on materials science) from the same University in 2004. This work was focused on the study of the electrical and magnetic properties of technological alloys and its relation with microstructure. Since 2001 Dr. Cano is a member of the research staff of the Laboratory of Materials (LEIM) at the Electrical Engineering School (EIE) of the Faculty of Science and Engineering (FCEIA) of the UNR. Since 2009 Dr. Cano is an Associate Professor of Electrical Machines and Power Systems at the Electrical Engineering School (EIE), FCEIA, UNR. Nowadays he is head of the Electrical Engineering School (EIE) from the same University. His research interest's areas include materials science and its applications.

Griselda Irene Zelada was born in Rosario, Argentina in 1963. She obtained the B.Sc. and MSc. (physics, 1990) degrees from the Rosario National University (UNR) and the Ph.D. degree in engineering (2008), focussed on materials science, from the same University. Dr. Zelada-Lambri is a member since 1998 of the research staff of the Laboratory of Materials (LEIM) at the Electrical Engineering School (EIE) of the Faculty of Science and Engineering (FCEIA), Institute of Physics of Rosario (IFIR) of the UNR - CONICET. Her current research areas include the mechanical properties of refractory metals and the mechanical and electrical properties of polymers.

Jose Ángel García was born in Bilbao, Spain in 1955. He obtained the B.Sc. and M.Sc. (Physics, 1977) from the University of the Basque Country. His Ph.D. degree work was realized at the J.J.Thompson Physical Laboratory of the Reading University in Great Britain. He spent several Post-Doctoral stages at Reading University and at the Science Faculty and Engineering of National University of Rosario in Argentina. At this time he is responsible of the Optical Emission Spectroscopy Laboratory of the Science Faculty in the Basque Country in Leioa.

David Merida Sanz was born in Eibar (Guipuzkoa), Spain in 1981. Graduated in physics (2006) from the University of the Basque Country. Pre-doctoral position in the laboratory of Nuclear techniques applied to Material Science at the Science and Technology Faculty of the UPV/EHU. In the last four years he has been in charge of the subject of "Fundamental Physics" at the Polytechnical College of San Sebastian.

Fernando Plazaola Muguruza was born in Legorreta (Gipuzkoa), Spain in 1958. Graduated in physics (1982) from the Complutense University of Madrid. He had a pre-doctoral position in the Laboratory of Physics of the Helsinki University of Technology (HUT), Finland between 1982-85. He obtained the Ph.D. degree in physics (1986, focussed on materials science) from the University of the Basque Country (UPV/EHU). He was a Guest Scientist at the Helsinki University of Technology (HUT) in 1997. Since 1998 he is Full Professor of Applied Physics at the University of the Basque Country. Since 1999 he is the head of the laboratory of Nuclear Techniques applied to Material Science at the Science and Technology Faculty of the UPV/EHU. He has been visiting Professor at HUT (2003). His current research areas include magnetic materials, defect studies in compound semiconductors and polymers.

Carlos Eugenio Boschetti was born in 1965 in Rosario, Argentina. He obtained his chemistry degree from the National University of Rosario (UNR) in 1991, and the Ph.D. degree (Chemistry) from the same University in 1995. He had post-doctoral positions at the Dept. of Organic Chemistry in the University of the Basque Country, Donostia, and then at the Dept. of Chemistry in the University of Cambridge, UK, as a Marie Curie Fellow (European Commission). After spending some time in the R+D Department of a petrochemical company, he gained in 2004 a position as Researcher in the National Council for Research and Technology of Argentina (CONICET). He has had many teaching positions in the Faculty of Biochemical and Pharmaceutical Sciences in the National University of Rosario, being currently an Associate Professor in the Chemical Technology Area at the same Faculty. His current research areas include analytical and process chemistry on polymers and polymerization.

Gerardo Esteban Martínez Delfa was born in Rosario, Argentina in 1980. He received his degree in chemistry from Rosario National University (UNR) in 2005 and the Ph.D. degree from the same university in 2010. His research is focused on the development of analytical techniques for the petrochemical and petroleum industry. His is currently working at the research center of YPF S.A. located in Ensenada, Buenos Aires.